J Nanopart Res (2013) 15:1443
DOI 10.1007/s11051-013-1443-6

RESEARCH PAPER

Statistical analysis of solid lipid nanoparticles produced by high-pressure homogenization: a practical prediction approach

Matilde Durán-Lobato · Alicia Enguix-González · Mercedes Fernández-Arévalo · Lucía Martín-Banderas

Received: 11 October 2012 / Accepted: 16 January 2013 / Published online: 1 February 2013

Abstract Lipid nanoparticles (LNPs) are a promising carrier for all administration routes due to their safety, small size, and high loading of lipophilic compounds. Among the LNP production techniques, the easy scale-up, lack of organic solvents, and short production times of the high-pressure homogenization technique (HPH) make this method stand out. In this study, a statistical analysis was applied to the production of LNP by HPH. Spherical LNPs with mean size ranging from 65 nm to 11.623 μm, negative zeta potential under –30 mV, and smooth surface were produced. Manageable equations based on commonly used parameters in the pharmaceutical field were obtained. The lipid to emulsifier ratio ($R_{L/S}$) was proved to statistically explain the influence of oil phase and surfactant concentration on final nanoparticles size. Besides, the homogenization pressure was found to ultimately determine LNP size for a given $R_{L/S}$, while the number of passes applied mainly determined polydispersion. α-Tocopherol was used as a model drug to illustrate release properties of LNP as a function of particle size, which was optimized by the regression models. This study is intended as a first step to optimize production conditions prior to LNP production at both laboratory and industrial scale from an eminently practical approach, based on parameters extensively used in formulation.

Keywords Solid lipid nanoparticles · High-pressure homogenization · Statistical analysis · Regression model · Particle size prediction · Mathematical model · Drug release

M. Durán-Lobato (✉) · M. Fernández-Arévalo · L. Martín-Banderas
Dpto. Farmacia y Tecnología Farmacéutica, Facultad de Farmacia, Universidad de Sevilla, C/Prof. García González n°2, 41012 Seville, España
e-mail: mduran@us.es

A. Enguix-González
Dpto. Estadística e Investigación Operativa, Facultad de Matemáticas, Universidad de Sevilla, C/Tarfia s/n, 41012 Seville, España

Introduction

Solid lipid nanoparticles (LNPs) consist of carrier systems made from lipids in which drug compounds can be incorporated. Their mean particle size is in the submicron range, ranging from about 40 to 1,000 (nm). Particle matrix is made of a solid lipid or a blend of solid lipids, aiming for accurate encapsulation and delivery of compounds (Pardeike et al. 2009). These carrier systems adopted some of the best features of other colloidal carriers such as polymeric nanoparticles and liposomes and can be made of physiological lipids (biocompatible and biodegradable), which support their safety (Müller et al. 2000b). Their small particle size allows them to be used for all routes of

administration (Souto and Müller 2006; Bondì et al. 2010; Müller et al. 1997). In addition, they have shown high encapsulation rates for lipophilic compounds (Das and Chaudhury 2011).

Several different methods for the production of LNP have been described in the literature. These methods are high-pressure homogenization technique (HPH, Liedtke et al. 2000; Mehnert and Mäder 2001), microemulsion technique (Gasco 1997; Priano et al. 2007), emulsification–solvent evaporation method (Sjöstrom and Bergenstahl 1992), emulsification–solvent diffusion method (Hu et al. 2002; Trotta et al. 2003), solvent injection (or solvent displacement) method (Schubert and Müller-Goymann 2003), phase inversion method (Heurtault et al. 2002), multiple emulsion technique (García-Fuentes et al. 2002), ultrasonication technique (Puglia et al. 2008), membrane contactor technique (Charcosset et al. 2005; El-Harati et al. 2006), supercritical fluid technique (supercritical fluid extraction of emulsions Chattopadhyay et al. 2007, and gas-assisted melting atomization Salmaso et al. 2009) and spray drying technique (Sebti and Amighi 2006).

However, the lack of a large-scale production method yielding a product of a quality that is acceptable by the regulatory authorities (e.g., Food and Drug Administration) generally hinders the introduction of solid nanoparticles to the market. This lack is due to basic technological problems (e.g., basic scale-up problem, toxicologically problematic residues from the production process) and regulatory aspects such as suitability of the production unit and production process to be qualified and validated (Müller et al. 2000a). Considering this, the lack of organic solvents, short production times, and easy scale-up provided by the HPH technique make this method highly suitable (Liedtke et al. 2000; Mehnert and Mäder 2001; Mucho et al. 2008). Either the hot or cold HPH technique can be applied to obtain LNPs, enabling to adapt the production according to the physicochemical properties of compounds and the behavior expected from the particles (Zur Mühlen et al. 1998; Zur Mühlen and Mehnert 1998). Furthermore, high-pressure homogenizers are widely used in many industries including the pharmaceutical industry, e.g., for the production of emulsions for parenteral nutrition. Hence, no regulatory problems exist for the production of LNP using this production technique, which can be considered as being industrially the most feasible one (Müller et al. 2000a).

LNP production methods including HPH present, however, certain hurdles that affect the product quality, i.e., drug degradation induced during the manufacturing process, lipid crystallization, gelation phenomena, supercooled melts, lipid and particle shape modifications, and the co-existence of several colloidal species (Mishra et al. 2012; Sinha et al. 2010). Nevertheless, these limitations can be overcome by monitoring the production conditions (temperature range, shear stress, light) and improving the selection of the drug carrier, the formulation, and the drug loading technique (Mishra et al. 2012; Sinha et al. 2010). Therefore, whatever production technique is used, identifying and optimizing the parameters influencing the final product is of paramount importance, since these determine the drug delivery system properties. Nowadays, the use of experimental designs has become a common method to simultaneously analyze the influence of different variables on the production of particles (Araujo et al. 2010; Varshosaz et al. 2010), especially regarding size (Vitorino et al. 2011). In the case of HPH, many thorough studies focused on emulsions and the homogenization process itself has been carried out (Mohr 1987a, b; Floury et al. 2000; Qian and McClements 2010; Maindarkar et al. 2012), but fewer attended to LNP (Severino et al. 2012).

In this study, a statistical analysis is applied to the production of LNPs by HPH technique from a completely practical approach. A wide range of pressure values, excipient concentrations, and number of passes are analyzed. Commonly employed parameters are used to describe the process, leading to manageable equations predicting particle size. The influence of particle size on the final properties of the delivery system is further illustrated using tocopherol as a model drug.

Experimental

Materials

Glycerol monostearate (Monostearin, melting point 63–68 °C, Acofarma, Spain) was used as lipid base. Sorbitan monostearate (Span® 60), polysorbate 80 (Tween® 80), and α-tocopherol were supplied by Sigma-Aldrich (Spain). Dihydrogen sodium phosphate and phosphoric acid were provided by Panreac

(Spain). Acetonitrile (high performance liquid chromatography [HPLC] gradient) was supplied by VWR (Spain). Distilled water was used for all the formulations.

LNP preparation

LNPs were prepared by HPH as described elsewhere (Zur Mühlen et al. 1998). Oil-in-water emulsions were prepared by dispersing 0.5 %, 2.5 %, 5.0 %, 7.5 %, 10 %, 15 % w/v of lipid in distilled water with emulsifier at a concentration of 0.12 %, 0.25 %, 0.5 %, 1.0 %, 1.25 %, 1.5 % (w/v) for each lipid concentration assayed, yielding a total number of 6^2 formulations. A dispersing step *prior to* homogenization was performed with an Ultra-Turrax (IKA®-WERKE, Germany) at 75 °C. The systems obtained were passed through a homogenizer (Panda 2K, Gea Niro Soavi, Italy) for different number of passes (1–8) at various homogenization pressures (250–1,500 bar). On account of technical recommendation (Gea Niro Soavi) and in order to prevent drop recoalescence, pressure at the second valve was fixed at relations 1:5 and 1:10 referred to total pressure for values lower and higher than 600 bar of final pressure, respectively. Samples' temperature variations due to pressure were monitored. In the case of α-tocopherol-loaded LNP, the compound was solubilized in the oil phase of initial emulsions at a concentration of 10 % (w/w) referred to the lipid matrix.

LNP characterization

Mean particle size and particle size distribution were measured by a laser scattering technique based on Mie theory (LA-950V2 Horiba, Japan) at 25 ± 0.5 °C. Measurements were carried out under continuous magnetic agitation. Measure range was fixed between 0.01 and 3,000 μm. Samples were measured directly or after dilution with distilled water when necessary.

LNP surface charge was determined by zeta potential (ZP) measurements. Particles ZP was determined by laser Doppler (Zetamaster 300, Malvern Instruments Ltd, Malvern, UK) at 25 ± 0.5 °C. ZP measurements were carried out in triplicate. Samples were measured directly or after dilution with distilled water when necessary.

LNP morphology and surface were characterized by image analysis obtained by scanning electron microscopy (SEM). For this purpose, a drop of LNP dispersion was spread on carbon tab previously stuck to aluminum stubs and dried overnight. Samples were coated with gold using a sputter coater (EDWARDS Scancoat Six) and examined in a Jeol 6460LV. Besides, particles were also observed by transmission electron microscopy (TEM). In this case, a drop of LNP dispersion was spread on a carbon-coated 200-mesh copper grid and dried overnight. Then, a drop of 2 % (w/v) uranyl acetate in ethanol was placed onto the grid for 10 min, followed by a drop of 2 % (w/v) lead citrate for 15 min. The grid was dried at room temperature and later observed in a Philips CM-10 (Philips, Germany).

Statistical analysis

All measurements were performed by triplicate on fresh samples also prepared by triplicate. An initial statistical evaluation of data was carried out by one-way analysis of variance. Statistical analysis was considered significant if the p values were lower than 0.05. Further statistical analysis was performed using PASW Statistics 18 (SPSS Inc., 2010).

Entrapment efficiency and loading capacity

Considering the entrapment efficiency (EE) the amount of drug that can be incorporated into the particles, and considering the loading capacity (LC) the amount of drug incorporated per mg of lipid, both parameters were calculated according to the following equations:

$$\mathrm{EE}\,(\%) = \frac{\text{Incorporated tocopherol (g)}}{\text{Total tocopherol (g)}} \times 100,$$

$$\mathrm{LC}\,(\%) = \frac{\text{Incorporated tocopherol (g)}}{\text{Amount of lipid (g)}} \times 100.$$

The amount of drug contained in the samples was measured by reverse phase HPLC with spectrophotometric detection according to a previously published method (Trombino et al. 2009) with some modification. Briefly, 4–5 mg of LNPs were accurately weighed and dissolved in 100 μL DCM. After 10 min of sonication, 900 μL of mobile phase was added, and samples were sonicated again for 5 min. Then, samples were filtered by 420 nm filter and injected into HPLC system. A 1-cm cartridge precolumn with 5-μm C18 Adsorbosphere packing was used.

Mobile phase consisted of 0.01 M dihydrogen sodium phosphate/0.01 M phosphoric acid with acetonitrile (88:12, v/v) pH 2.3, at a flow rate of 0.5 mL/min. Wavelength was fixed at 280 nm on a Jasco UV-2075 detector.

Drug release from LNP

In order to study the drug release from the particles, LNP samples were suspended in phosphate buffer (pH 7.4) containing Tween® 80 at a concentration of 0.1 % (w/v), maintained at 37 °C and stirred mechanically (100 rpm) during the release experiments (Unitronic OR, Selecta, Spain). Aliquots (500 µL) were withdrawn at fixed time intervals and filtered upon centrifugation at 8,000 rpm. Filtered samples (Millex GV) (10 µL) were injected into the HPLC equipment to quantify the amount of α-tocopherol.

Table 1 Values of applied pressure and corresponding formulation temperature and mean particle size obtained by laser scattering

Homogenization pressure (bar)	Mean diameter ± SD (µm)	CV (%)	Formulation mean temperature ± SD (°C)
300	2.990 ± 2.263	74.40	41 ± 1
500	1.580 ± 1.524	96.45	43 ± 1
800	0.810 ± 0.694	85.58	48 ± 0
1,000	0.241 ± 0.226	93.52	51 ± 1
1,300	0.124 ± 0.049	39.46	61 ± 1
1,500	0.093 ± 0.030	37.01	67 ± 1

Results and discussion

LNP characterization

The influence of lipid concentration, surfactant concentration, applied pressure, and number of passes on mean particle size and size distribution was studied. Mean particle size ranged from 65 nm to 11.623 µm. The applied pressure proved to be a high influencing parameter on particle size and size distribution (Table 1), leading to a decrease in LNP size as the pressure was increased. The number of passes applied induced a strong decrease in particle size and size distribution as well, which changed from bimodal to monomodal as the number of cycles was increased (Fig. 1). Temperature was monitored for each pass at every value of pressure (Table 1), remaining constant for each value of pressure regardless of the number of passes applied and formulation composition. An increase in surfactant concentration led to a decrease in LNP size, while increasing both surfactant and lipid concentrations in a constant relationship did not induce significant changes in particle size (Fig. 2). Since the influence of these parameters was statistically analyzed and mathematically described, these results will be further commented in the "Statistical analysis" section. Incorporation of tocopherol did not influence particle size distribution (data not shown).

ZP of all samples was under -30 mV, thus indicating the suspensions were stable a priori.

SEM imaging showed spherical particles with a smooth surface (Fig. 3). However, only large-sized particles could be observed by SEM, since the voltage needed to capture the smallest particles was extremely

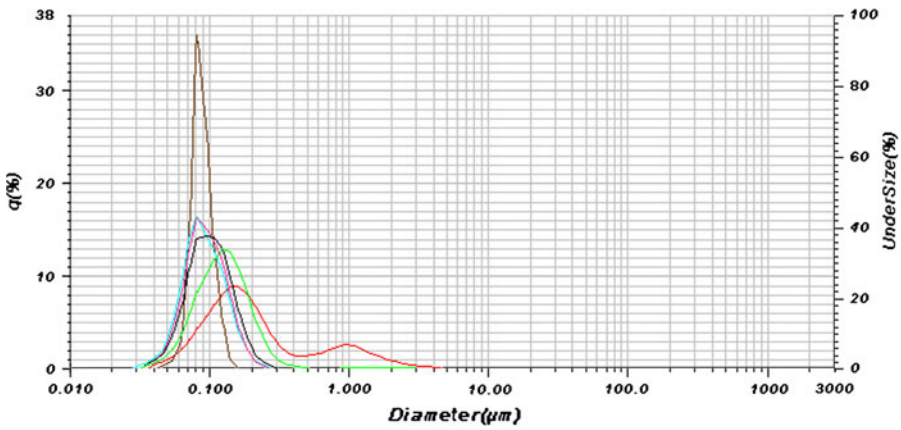

Fig. 1 LNP size distributions of formulations produced at 1,500 bar of pressure with 0.5 % (w/v) of Monostearin and 0.5 % (w/v) of Span® 60 after: *red* one homogenization cycle, *green* two homogenization cycles, *dark blue* three homogenization cycles, *magenta* four homogenization cycles, *light blue* five homogenization cycles, *brown* six homogenization cycles. (Color figure online)

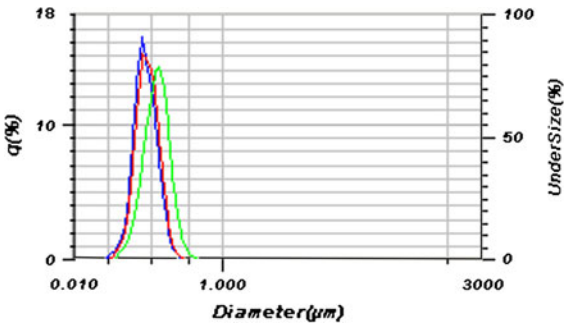

Fig. 2 LNP size distribution of formulations produced with: *blue* 0.50 % (w/v) of Monostearin and 0.25 % (w/v) of Span® 60; *red* 2.50 % (w/v) of Monostearin and 1.25 % (w/v) of Span® 60; *green* 10.00 % (w/v) of Monostearin and 5.00 % (w/v) of Span® 60. (Color figure online)

high and made them melt. Thus, TEM was applied to confirm the size of the smallest particles. Transmission images enabled to observe particles smaller than 500 nm (Fig. 4), confirming therefore the experimental results. No morphological differences were found between empty and tocopherol-loaded LNP.

Statistical analysis

Statistical analysis of data was structured in separate stages. First, functional values of production conditions were tested to determine the operating range where the equipment performance, and hence the obtained data, were reliable. Maximal pressure value was fixed at 1,500 bar on account of technical

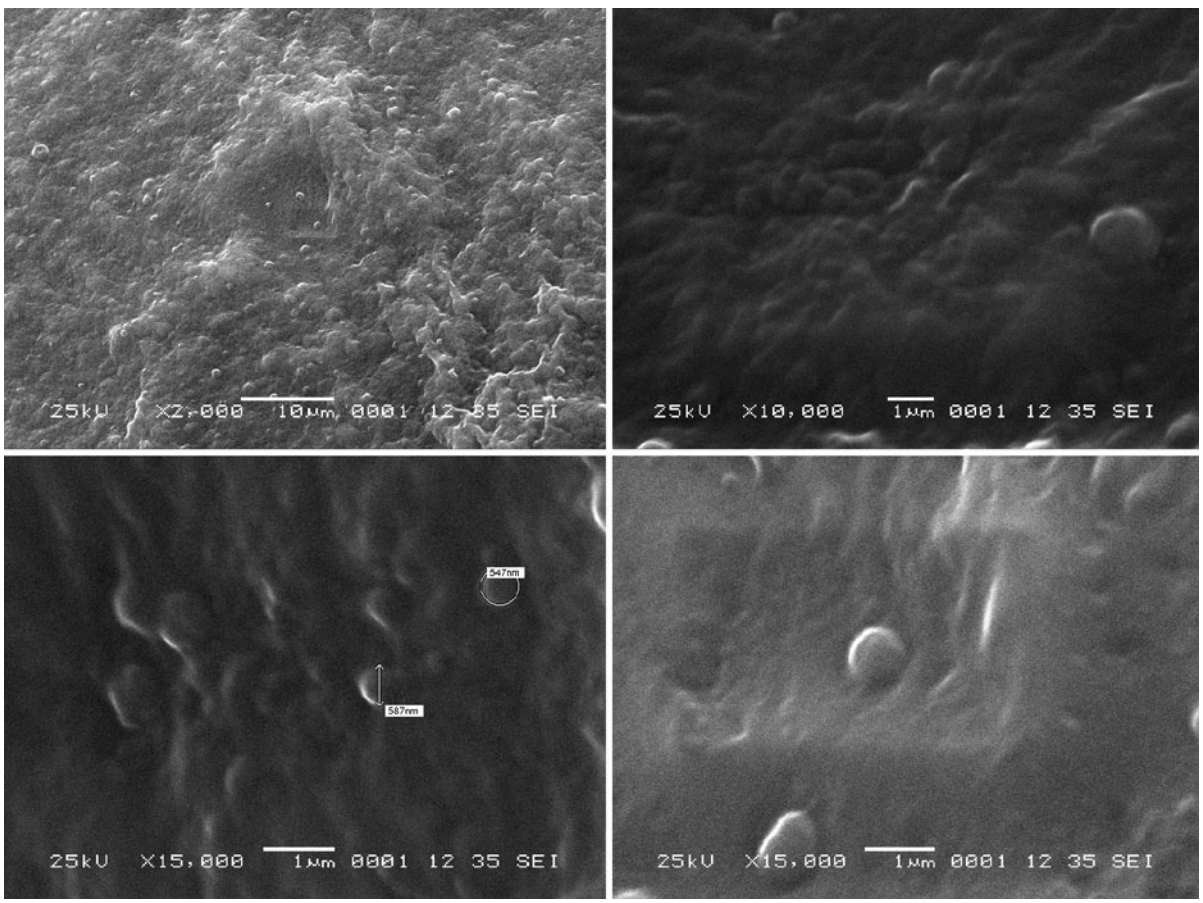

Fig. 3 SEM images of LNP formulations. From *left* to *right*, *top* to *bottom* particles produced with 10.00 % (w/v) of lipid and 1.25 % (w/v) of emulsifier at 800 bar and five cycles; particles produced with 2.50 % (w/v) of lipid and 0.25 % (w/v) of emulsifier at 800 bar and five cycles; particles produced with 2.50 % (w/v) of lipid and 0.12 % (w/v) of emulsifier at 1,000 bar and five cycles; particles produced with 0.25 % of α-tocopherol, 2.50 % (w/v) of lipid, and 0.25 % (w/v) of emulsifier at 800 bar and six cycles

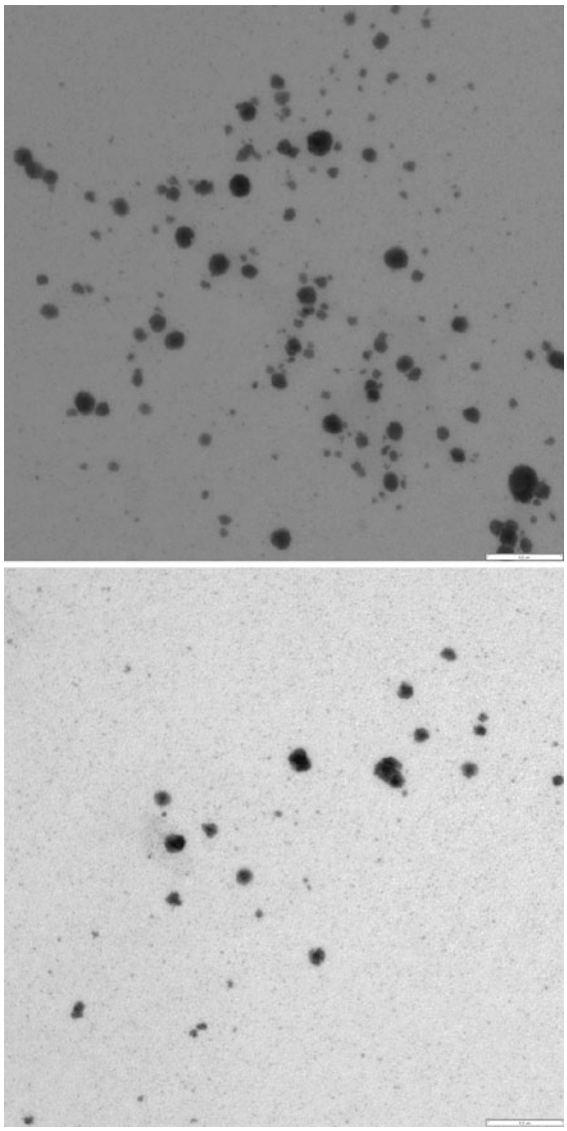

Fig. 4 TEM images of LNP formulations. From *top* to *bottom*, particles produced with 2.50 % (w/v) of lipid and 1.25 % (w/v) of emulsifier at 1,500 bar and five cycles; particles produced with 0.50 % (w/v) of lipid and 0.5 % (w/v) of emulsifier at 1,500 bar and eight cycles

recommendation (Gea Niro Soavi). Lipid concentrations were kept under 15 % (w/v), since higher values yielded low-fluid emulsions that could block homogenizer channels. Finally, maximal surfactant concentration was fixed at 1.5 % (w/v) to prevent the formation of bubbles inside the equipment. Following, and since there were no major differences between intermediate values, six values from each of the above variables were selected; 300, 500, 800, 1,000, 1,300, 1,500 bar of pressure; 0.5 %, 2.5 %, 5.0 %, 7.5 %, 10 %, 15 % (w/v) lipid concentrations; 0.12 %, 0.25 %, 0.5 %, 1.0 %, 1.25 %, 1.5 % (w/v) emulsifier concentrations. A design similar to Latin square was applied to ensure representativeness in the combination of values from production conditions, with 288 measures from 36 batches and eight passes, which provided a total number of 458 valid measures of particle size.

Secondly, and prior to the study of data, outlier detection techniques were applied in order to debug the data and thus guarantee the quality of the results.

Finally, mathematical description of mean and mode size from values of applied pressure, surfactant and lipid concentrations, and number of passes was performed. The study of regression models for mode size prediction was motivated by the changes observed in size distribution when consecutive homogenization passes were applied (Fig. 1) and the bimodal distributions occurred frequently. Production conditions were taken as dependent variables and were represented in the mathematical models either by itself or through mathematical transformation. The determination coefficient R^2 was used as indicative of the accuracy of the adjustment from each variable as well as from the global equations, and was therefore used to discriminate between the models. Linear, polynomial, logarithmic, inverse, exponential, and growing models were considered, among others. Additive models were finally chosen on account of their simplicity and goodness of fit, involving up-to-fourth-degree-polynomial, logarithmic and exponential regression models, either with direct and/or inverse terms. They were simplified as much as possible to eliminate terms with low contributions to the models according to R^2 values. In general, polynomial terms of higher degree than quadratic functions, exponential and logarithmic terms were unnecessary. Final proposed regression models are presented in Table 2a, b. These simpler models, nearly equivalent to others of more complex adjustment, describe the relationship among the studied variables and particle size quickly and clearly. Moreover, these manageable regression models allow predicting particle size from initial conditions controlled by the experimenter directly, since independent variables are represented in the equations by common parameters used in formulations.

Table 2 Proposed models of mean (d_{mean}) (a) and mode (d_{mode}) (b) particle size and its determination coefficients R^2 for each cycle studied

Cycles	R^2	Proposed model
a		
1	0.737	$d^{C1}_{mean} = 0.357 - \frac{1.432}{L} + \frac{2.81}{P^*}$
2	0.821	$d^{C2}_{mean} = 2.797 - 0.604S - 1.559P^* - \frac{0.9832}{L} + \frac{1.344}{P^*}$
3	0.831	$d^{C3}_{mean} = 2.112 - 1.535P^* - \frac{0.27}{L} - \frac{0.492}{R_{L/S}} + \frac{1.027}{P^*}$
4	0.887	$d^{C4}_{mean} = 1.389 - 1.046P^* - \frac{0.377}{R_{L/S}} + \frac{0.583}{P^*}$
5	0.783	$d^{C5}_{mean} = -0.074 - \frac{0.184}{R_{L/S}} + 0.882P^{*2} - \frac{0.172}{P^{*2}} - 3.973 \log P^*$
6	0.948	$d^{C6}_{mean} = -0.311 - \frac{0.323}{R_{L/S}} + \frac{0.887}{P^*}$
7	0.939	$d^{C7}_{mean} = -0.31 - \frac{0.299}{R_{L/S}} + \frac{0.83}{P^*}$
8	0.945	$d^{C8}_{mean} = -0.307 + \frac{0.78}{P^*} - \frac{0.307}{R_{L/S}}$
b		
1	0.722	$d^{C1}_{mode} = 2.149 - 0.822P^{*2} - \frac{0.09}{R^2_{L/S}}$
2	0.268	
3	0.832	$d^{C3}_{mode} = 2.677 - 1.743P^* - \frac{0.1}{R^2_{L/S}}$
4	0.839	$d^{C4}_{mode} = 2.632 - 1.71P^* - \frac{0.1}{R^2_{L/S}}$
5	0.888	$d^{C5}_{mode} = 0.707 - 1.52 \log P^* - \frac{0.094}{R^2_{L/S}}$
6	0.894	$d^{C6}_{mode} = 0.672 - 1.371 \log P^* - \frac{0.096}{R^2_{L/S}}$
7	0.866	$d^{C7}_{mode} = 0.647 - 1.251 \log P^* - \frac{0.094}{R^2_{L/S}}$
8	0.833	$d^{C8}_{mode} = 0.627 - 1.182 \log P^* - \frac{0.093}{R^2_{L/S}}$

No regression models for mode size were found to fit the data adequately for the second cycle

$d^{C(1-8)}$, particle size for cycles 1–8; P^*, final applied pressure (kbar); L, lipid concentration (% w/v); S surfactant concentration (% w/v); $R_{L/S}$, ratio of lipid concentration to surfactant concentration (L/S)

A summary of R^2 values obtained from the variables and their mathematical transformations employed for the generation of the models can be found in Table 3. The implication of each variable in the process and the extent of their influence revealed in the models will be further discussed regarding the production process.

Overall, the mean size of the nanoparticles can be explained through its logarithm by the following model (1):

$$\log d_{mean} = 3.203 - 2.691P^* - 0.21 \text{ cycle} - \frac{0.398}{R_{L/S}} \quad R^2 = 0.8490, \quad (1)$$

where d_{mean} is the mean particle size, P^* is the applied pressure (kbar), cycle is the number of passes applied, and $R_{L/S}$ is the ratio of lipid concentration referred to surfactant concentration. This equation was obtained following the process described above for the generation of the models set out in Table 2a, b. Natural logarithm of the mean particle size was considered the dependent variable, and the rest of experimental conditions and their mathematical transformations were taken as independent variables. Once again, R^2 was taken as reference for the selection of terms according to their contribution to the adjustment.

Since formulation temperature remained under the lipid melting point throughout the homogenization process, the intermediate products should be considered as suspensions. However, due to the similarities between the results obtained in this study and published data about emulsions, references on both kind of systems, lipid suspensions and emulsions, will be commented in this study. A direct and stronger influence of homogenization pressure over temperature in homogenized O/W emulsions was also reported by Floury et al. (2000).

When studying the HPH process, it is worth mentioning that the HPH technique has been theoretically and experimentally analyzed. Originally, two stages were mechanistically differentiated in the process. According to this, primary dispersion is affected by the energy of large eddies formed in a turbulent flow. Secondary dispersion takes place by viscous shearing between convergent small eddies in the case of very high energy densities (Mohr 1987b). Considering these mechanisms, particles deformation is proportional to the system energy which is directly related to the pressure. Later, both turbulence and viscous shearing mechanisms were considered to happen simultaneously, depending on the system composition, its energy and thus pressure. Initially, inertial forces dominate the process and droplets break up due to pressure fluctuations from turbulence. This process is described by Eq. (2) (Walstra 1993) where d_{max} is the maximum droplet diameter (m), C is a constant (–), ε is power density (W m^{-3}), γ is interfacial tension (N m^{-1}), and ρ is mass density (kg m^{-3}):

Table 3 Values of correlation coefficient in decreasing order, in absolute terms, between d_{mean} and P^*, final applied pressure (kbar); L, lipid concentration (% w/v); S, surfactant concentration (% w/v); $R_{L/S}$, ratio of lipid concentration to surfactant concentration (L/S), and transformations of them

Cycle 1		Cycle 2		Cycle 3		Cycle 4		Cycle 5		Cycle 6		Cycle 7		Cycle 8	
Variable	r	Variable	r	Variable	r	Variable	r	Variable	r	Variable	r	Variable	r	Variable	r
$1/P^*$	0.758	$\log P^*$	−0.652	$\log P^*$	−0.803	$\log P^*$	−0.778	$\log P^*$	−0.873	$1/P^*$	0.912	$1/P^*$	0.927	$1/P^*$	0.925
$\log P^*$	−0.751	P^*	−0.644	P^*	−0.785	P^*	−0.769	$1/P^*$	0.852	$\log P^*$	−0.895	$\log P^*$	−0.915	$\log P^*$	−0.908
$1/P^{*2}$	0.733	$1/P^*$	0.618	$1/P^*$	0.773	$1/P^*$	0.739	P^*	−0.847	$1/P^{*2}$	0.892	$1/P^{*2}$	0.904	$1/P^{*2}$	0.907
P^*	−0.71	$\exp(P^*)$	−0.612	$\exp(P^*)$	−0.745	$\exp(P^*)$	−0.733	$\exp(P^*)$	−0.802	$\exp(1/P^*)$	0.863	$\exp(1/P^*)$	0.871	$\exp(1/P^{*3})$	0.879
$\exp(1/P^*)$	0.699	P^{*2}	−0.609	P^{*2}	−0.74	P^{*2}	−0.729	P^{*2}	−0.796	$1/P^{*3}$	0.862	$1/P^{*3}$	0.87	$\exp(1/P^*)$	0.88
$1/P^{*3}$	0.698	P^{*3}	−0.567	$1/P^{*2}$	0.71	P^{*3}	−0.683	$1/P^{*2}$	0.794	P^*	−0.84	P^*	−0.86	$1/P^{*4}$	0.855
$1/P^{*4}$	0.668	$1/P^{*2}$	0.555	P^{*3}	−0.69	$1/P^{*2}$	0.668	P^{*3}	−0.743	$1/P^{*4}$	0.835	$1/P^{*4}$	0.842	P^*	−0.85
P^{*2}	−0.656	P^{*4}	−0.53	$1/P^{*3}$	0.646	P^{*4}	−0.641	$1/P^{*3}$	0.731	$\exp(P^*)$	−0.78	$\exp(P^*)$	−0.799	$\exp(P^*)$	−0.786
$\exp(P^*)$	−0.664	$1/P^{*3}$	0.493	P^{*4}	−0.646	$1/P^{*3}$	0.598	$\exp(1/P^*)$	0.731	P^{*2}	−0.771	P^{*2}	−0.789	P^{*2}	−0.776
P^{*3}	−0.607	$\exp(1/P^*)$	0.492	$\exp(1/P^*)$	0.645	$\exp(1/P^*)$	0.597	$1/P^{*4}$	0.683	P^{*3}	−0.71	P^{*3}	−0.726	P^{*3}	−0.709
P^{*4}	−0.566	$1/P^{*4}$	0.447	$1/P^{*4}$	0.597	$1/P^{*4}$	0.545	P^{*4}	−0.697	P^{*4}	−0.663	P^{*4}	−0.675	P^{*4}	−0.656
$1/L$	−0.376	$1/R^4_{L/S}$	0.33	$\log R_{L/S}$	0.148	$1/R^4_{L/S}$	0.157	$1/R^4_{L/S}$	0.149	$\log R_{L/S}$	0.226	$\log R_{L/S}$	0.223	$\log R_{L/S}$	0.271
⋮	⋮	⋮	⋮	⋮	⋮	⋮	⋮	⋮	⋮	⋮	⋮	⋮	⋮	⋮	⋮
$1/R^3$	−0.002	$1/S^2$	0.011	S^4	−0.009	$1/L^4$	−0.003	$\log L$	0.004	$1/R^3$	−0.019	$1/R^3$	−0.024	$1/R^3$	−0.025

$$d_{\max} = C\varepsilon^{-2/5}\gamma^{3/5}\rho^{-1/5}. \quad (2)$$

Shearing mechanisms predominate when viscosities increase, leading to larger particle sizes and wider distributions (Walstra 1993). In this case, droplets break up due to shear stress, and size follows Eq. (3) where η_c is the viscosity of the continuous phase:

$$d_{\max} = C\gamma\varepsilon^{-1/2}\eta_c^{-1/2}. \quad (3)$$

In addition, impact mechanisms and the influence of cavitation, although less influencing than turbulence and shearing mechanisms, were considered relevant in the dispersing process (Floury et al. 2000; Mohr 1987a; Håkansson et al. 2011), both effects being dependent on pressure. However, an enhancing effect on emulsification by means of back pressure would be later considered as suppression of collapse cavitation in the high-pressure emulsification module (Saheki et al. 2012).

More recently, the experimental effect of HPH on droplet size distribution has been intensely studied on micro- and nanoemulsions from food industry, mainly on dairy products. All the investigations showed unanimously a decrease in particle size when a higher pressure was applied (Floury et al. 2000; Qian and McClements 2010; Innocente et al. 2009; Biasutti et al. 2010). More specifically, a logarithmic relationship between droplet size and pressure applied was defined by Qian and McClements (2010), for an emulsion with 5 % v/v of oil internal phase after six passes of homogenization as follows:

$$\log(d/\text{nm}) = -0.289\log(P/\text{kbar}) + 2.499 \qquad R^2 = 0.9938, \quad (4)$$

where d is droplet diameter (nm) and P the applied pressure (kbar), and a linear relationship in Severino et al. (2012) for a formulation with 10 % (w/w) lipid and 5 % (w/w) of total emulsifier is as follows:

$$\text{Particle size (nm)} = -8.9750P, \quad (5)$$

where P is HPH pressure of HPH (500, 700, and 900 bar of pressure, 1–3 cycles). These mathematical relationships are in accordance with the regression models exposed in this study. Furthermore, the highest values of correlation coefficient R^2 in absolute terms of the variables studied were obtained for the pressure term, either directly or through mathematical transformation (Table 3). Hence, the applied pressure was proved to be the most influencing parameter on particle size and size distribution, leading to a decrease in LNP size as the pressure was increased (Fig. 5). This fact is clearly reflected in all of the models.

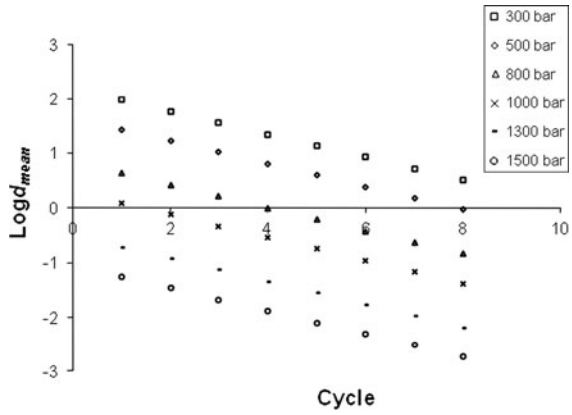

Fig. 5 Particle size as a function of number of cycles for a formulation with 0.5 % (w/v) of Monostearin and 0.25 % (w/v) of emulsifier (ratio $R_{L/S} = 2$), produced at different homogenization pressures (bar)

The formulation composition proved to be another variable significantly affecting regression models. According to published literature, higher fat contents in emulsions led to higher particle sizes (Floury et al. 2000; Innocente et al. 2009). A relative increase in the turbulent viscous mechanism over the turbulent inertial mechanism when increasing the volume fraction of dispersed phase, and hence an increase in droplet size, was also indicated (Håkansson et al. 2011). However, some experiments showed no important influence (Biasutti et al. 2010). In the meantime, increasing the concentration of emulsifier was reported to lead to smaller droplets as expected from the Eq. (5) (Walstra 1993). In the present study, the influence of the relationship between lipid and emulsifier concentration $R_{L/S}$ on particle size was found to be stronger than the influence of lipid or surfactant concentration separately (Table 2; Fig. 6). This possibly explains these disagreements in the published literature, and is supported by (McClements 2005), where the influence of fat content related to surfactant load was mathematically assessed as described in Eq. (6):

$$d_{\min} = \frac{6\Gamma\phi}{C_s} = \frac{6\Gamma\phi}{C_s'(1-\phi)}, \quad (6)$$

where $d_{\min}$ is the minimum size of stable droplets that can be produced during homogenization, Γ is the

surface load of emulsifier (kg m^{-2}), ϕ is the disperse phase volume fraction, C_s is the concentration of emulsifier in the emulsion (kg m^{-3}), and C_s' is the concentration of emulsifier in the continuous phase (kg m^{-3}). In fact, it was reported by Araujo et al. (2010) that the ultimate diameter of emulsion and liposomes is physicochemically determined by the composition ratio of oil to emulsifier phase. In the present study, a $R_{L/S}$ value of 1.0 allowed the production of LNP in the nanometer range under mild homogenization conditions (Fig. 6) and moderate emulsifier concentrations, which is generally the aim in most of the procedures. This may not be the $R_{L/S}$ of choice when different restrictions are present, e.g., the need of lower emulsifier concentrations to avoid purification issues or the demand of high lipid concentrations in order to incorporate an additional content of water in later steps (e.g., LNP incorporation into creams). In these cases, the optimal $R_{L/S}$ would be determined by formulation restrictions, and the rest of the parameters could be extrapolated from the models to obtain a similar LNP size and distribution.

The role of the type of emulsifier employed was studied as well, being reported that the decrease in particle diameter was appreciably different depending on the type of emulsifier used. This supports the trend that small-molecule surfactants are more effective in making small droplets than polymers or proteins (Walstra 1993; Qian and McClements 2010). The use of a different type of emulsifier should be analyzed in further studies with regard to the basic equations proposed in this study. There is also evidence in the literature of population balance equation (PBE) models of HPH predicting drop size distributions that are extensible to different surfactants if the adjustable model parameters were estimated based on chosen base case data (Maindarkar et al. 2012). Hence, the incorporation of information collected from experiences on other types of emulsifiers into the equation models in this study could open new possibilities.

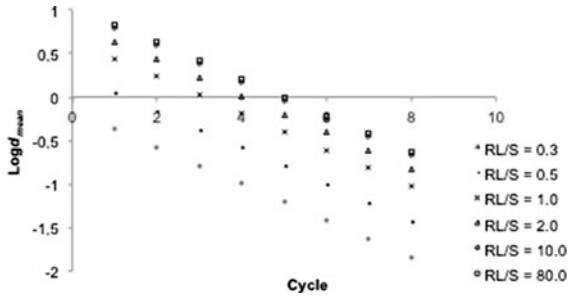

Fig. 6 Logarithm of mean LNP size from one to eight cycles of homogenization at 800 bar of pressure for each lipid to emulsifier ratio ($R_{L/S}$) employed

The role of the viscosity in the homogenization process should be considered as well. It was soon stated that an increase in the viscosity of the continuous phase η_c yielded an increase in particles size distribution (Mohr 1987b), which was later determined as in Eq. (3). Shearing mechanisms predominate when viscosities increase, leading to larger particle sizes and wider distributions (Walstra 1993; Håkansson et al. 2011). More studies showed droplet break-up becomes more difficult as the viscosity of the dispersed phase increases (Jafari et al. 2008; Qian and McClements 2010), hence leading to higher droplet diameters. Increasing the viscosity of the continuous phase induced a decrease in droplet diameter, suggesting that shear forces did play an important role in droplet disruption (Wooster et al. 2008; Qian and McClements 2010). In this study, no parameters regarding viscosity were included in the statistical analysis, since all formulations were elaborated with the same base lipid Monostearin. As in the case of the type of surfactant employed, different types of lipids should be employed in further studies for the adjustment of equations to a given formulation, and viscosity could be one of the most affected parameters. However, temperature formulation was initially assessed as an influencing variable at this point (Table 1), given that there is a strong warming up of the fluid due to viscous stress during the dispersing process (Floury et al. 2000). The viscosity of both oil and aqueous phases is temperature-dependent and decreases with increasing temperature. Consequently, the minimum droplet size that can be produced may be altered (Floury et al. 2000). Nonetheless, in this study, temperature proved to be highly correlated with the pressure and poorly correlated with the mean particle size when the pressure was included in the models, according to partial correlation coefficients. Considering that the pressure is a variable directly controlled by the experimenter and the temperature was measured posteriorly, the temperature was no longer considered in the statistical study.

Finally, the increasing number of cycles induced a decrease in mean particle size (Fig. 7) and, more

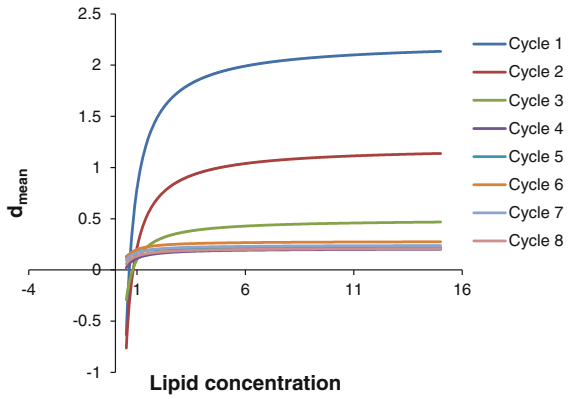

Fig. 7 Mean particle size of LNP produced at 1,500 bar of homogenization pressure and 0.25 % (w/v) of emulsifier as a function of lipid concentration, for different number of applied passes

markedly, in size distribution polydispersity (Fig. 1), as reported in published literature (Liedtke et al. 2000; Qian and McClements 2010). Specifically, and all in accordance with bibliography, the first pass produced a large decrease in particle size, while the following cycles produced reductions fairly modest. Mean droplet diameter did not change appreciably after certain number of passes (Qian and McClements 2010). On the other hand, different size distributions have been reported. Homogenization determined a change from bimodal to modal particle size distributions in ice cream mixes (Floury et al. 2000). This occurrence of bimodal distribution motivated the statistical study of mode size in this study, showing a statistically predictable behavior (Table 2b).

Nonetheless, the increasing number of homogenization cycles was reported to possibly contribute to particle aggregation and higher polydispersity (Severino et al. 2012; Liu et al. 2007) due to high kinetic energy of small particles. Moreover, the incorporation of coalescence into a PBE model of HPH under the form of collision functions was shown to provide superior predictions compared to the breakage-only model (Maindarkar et al. 2012), proving the influence of this phenomenon on the HPH process. In comparison, no appreciable influence of internal phase collisions was noticed in this study, which could be due to the application of pressure from the second valve. Another discordance in this study with literature concerns the optimal homogenization conditions to obtain a given particle size. Pressures of 500 bar and 1–3 passes are typically enough to obtain small particle sizes (Severino et al. 2012; Zur Mühlen et al. 1998) for which higher pressures and number of cycles were needed in this study. This could be attributed to the higher droplet sizes of coarse pre-emulsions that are produced under the conditions employed in this study. Furthermore, maintaining the working temperature under the base lipid melting point could contribute to these differences. HPH of suspensions showed similar behaviors to those previously exposed, regarding pressure and number of cycles influence and the evolution of bimodal distributions (Kluge et al. 2012).

In view of all the variables analyzed in this study, it could be deduced that, for a given lipid to surfactant ratio, the homogenization pressure determined the ultimate particle size, while the number of passes applied determined the polydispersity of that size distribution.

EE and LC

Drug content of tocopherol-loaded LNP was analyzed with regard to particle size. The results are shown in Table 4. Almost complete loading of tocopherol was achieved for all particle sizes studied, with EE values over 99 % and 10 % of LC. This can be attributed to the fact that tocopherol is a highly lipophilic drug (log *P* 9.959) and thus has a high affinity toward lipid matrix. In addition, particle size did not influence tocopherol loading capacity for the range of drug concentrations assayed.

Table 4 Tocopherol-loaded LNP size, production conditions (*L* lipid concentration, $R_{L/S}$ lipid to emulsifier ratio, *P* homogenization pressure (bar)) and corresponding values of encapsulation efficiency (EE) (%) and LC (%)

L (% w/v)	$R_{L/S}$	*P** (bar)	Cycle	Mean size (nm)	EE (%)	LC (%)
0.50	1	1,500	8	71 ± 8	91 ± 9	9 ± 1
0.50	2	1,300	5	188 ± 10	96 ± 5	8 ± 2
0.50	2	1,000	6	305 ± 12	94 ± 9	10 ± 2
2.50	20	1,000	6	487 ± 15	98 ± 6	10 ± 1
2.50	20	1,000	5	608 ± 14	97 ± 7	9 ± 2
2.50	10	800	6	886 ± 18	92 ± 10	10 ± 2
0.50	2	800	6	994 ± 22	94 ± 7	7 ± 2

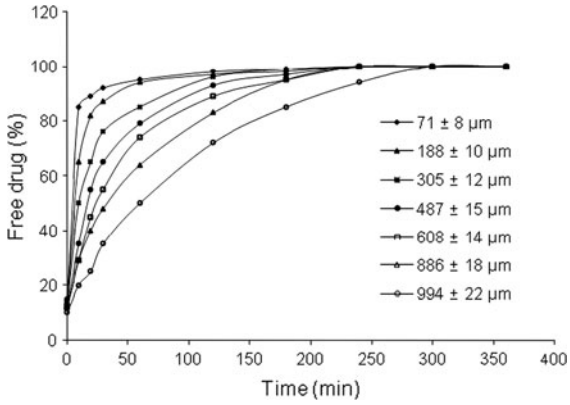

Fig. 8 Tocopherol release from LNP with 10 % of tocopherol LC as a function of particle size

Drug release from LNP

In order to study how particle size influences drug release from the nanoparticles, samples of tocopherol-loaded LNPs with different particle sizes but equal drug content were compared. The results of release studies are illustrated in Fig. 8. All formulations showed an initial burst release, probably due to drug and surfactant adsorbed onto particles surface and a drug shell-enriched structure of the nanoparticles (Schäfer-Korting et al. 2007). On one hand, the presence of surfactant was reported to accelerate drug release (Müller et al. 1994). On the other hand, a drug shell-enriched structure is typically obtained when the drug melting point is under the matrix lipid melting point, as in this case (2 °C for α-tocopherol; 63–68 °C for Monostearin). In the production process, lipid precipitation takes place first leading to a phase separation during the cooling process. The lipid occupies, therefore, the particle core while the compound is accumulated within the shell, reaching the release medium faster. Besides, it can be clearly appreciated that smaller particle sizes induced a faster release. This was expected since smaller sizes imply a higher contact surface of the particle with the external medium, so drug diffusion is favored. Consequently, a determined particle size should be achieved for a desired release, which can be easily done by means of the equations presented in this study.

Conclusions

LNPs are a promising drug delivery system for all administration routes. HPH is a highly advantageous LNP production technique at both laboratory and industrial scale. In this study, a statistical analysis was carried out aiming to understand and control the parameters influencing the production of LNP by HPH, and therefore their final properties. Manageable equations based on commonly used parameters in the pharmaceutical field were obtained. The lipid to emulsifier concentration ratio ($R_{L/S}$) was proved to statistically explain the influence of oil phase and surfactant concentration on final nanoparticles size. Besides, the homogenization pressure was found to ultimately determine LNP size for a given $R_{L/S}$, while polydispersion was mainly determined by the number of passes applied. Further studies regarding different lipids and types of emulsifier could extend the conditions covered by these regression models. This study is intended as a first step to optimize production conditions prior to LNP production at both laboratory and industrial scale from an eminently practical approach, based on extensively used parameters in formulation.

Acknowledgments M. D. L. thanks University of Seville for a Grant from IV Research Plan of University of Seville. L. M. B. is especially grateful to Junta de Andalucía (Spain) for financial support (Project No. P09-CTS5029). Microscopy Services (Centro de Investigación, Tecnología e Innovación de la Universidad de Sevilla, CITIUS) technical support is also grateful. Authors also thank Dr. Álvarez-Fuentes for technical support.

References

Araujo J, Gonzalez-Mira E, Egea MA, Garcia ML, Souto EB (2010) Optimization and physicochemical characterization of a triamcinolone acetonide-loaded NLC for ocular antiangiogenic applications. Int J Pharm 393:167–175

Biasutti M, Venir E, Marchesini G, Innocente N (2010) Rheological properties of model dairy emulsions as affected by high pressure homogenization. Innov Food Sci Emerg Technol 11:580–586

Bondì ML, Craparo EF, Giammona G, Drago F (2010) Brain-targeted solid lipid nanoparticles containing riluzole: preparation, characterization and biodistribution. Nanomedicine (Lond, Engl) 5:25–32

Charcosset C, El-Harati A, Fessi H (2005) Preparation of solid lipid nanoparticles using a membrane contactor. J Control Release 108:112–120

Chattopadhyay P, Shekunov BY, Yim D, Cipolla D, Boyd B, Farr S (2007) Production of solid lipid nanoparticle suspensions using supercritical fluid extraction of emulsions (SFEE) for pulmonary delivery using the AERx system. Adv Drug Deliv Rev 59:444–453

Das S, Chaudhury A (2011) Recent advances in lipid nanoparticle formulations with solid matrix for oral drug delivery. AAPS PharmSciTech 12:62–76

El-Harati AA, Charcosset C, Fessi H (2006) Influence of the formulation for solid lipid nanoparticles prepared with a membrane contactor. Pharm Dev Technol 11:153–157

Floury J, Desrumaux A, Lardières J (2000) Effect of high-pressure homogenization on droplet size distributions and rheological properties of model oil-in-water emulsions. Innov Food Sci Emerg Technol 1:127–134

García-Fuentes M, Torres D, Alonso MJ (2002) Design of lipid nanoparticles for the oral delivery of hydrophilic macromolecules. Colloid Surf B 27:159–168

Gasco MR (1997) Solid lipid nanospheres from warm microemulsion. Pharm Technol Eur 9:32–42

Håkansson A, Fuchs L, Innings F, Revstedt J, Trägårdh C (2011) On flow-fields in a high pressure homogenizer and its implication on drop fragmentation. Procedia Food Sci 1:1353–1358

Heurtault B, Saulnier P, Pech B, Proust JE, Benoit JP (2002) A novel phase inversion-based process for the preparation of lipid nanocarriers. Pharm Res 19:875–880

Hu FQ, Yuan H, Zhang HH, Fang M (2002) Preparation of solid lipid nanoparticles with clobetasol propionate by a novel solvent diffusion method in aqueous system and physicochemical characterization. Int J Pharm 239:121–128

Innocente N, Biasutti M, Venir E, Spaziani M, Marchesini E (2009) Effect of high-pressure homogenization on droplet size distribution and rheological properties of ice cream mixes. J Dairy Sci 92:1864–1875

Jafari S, Assadpoor E, He Y, Bhandari B (2008) Re-coalescence of emulsion droplets during high-energy emulsification. Food Hydrocoll 22:1191–1202

Kluge J, Muhrer G, Mazzotti M (2012) High pressure homogenization of pharmaceutical solids. J Supercrit Fluids 66:380–388

Liedtke S, Wissing S, Müller RH, Mäder K (2000) Influence of high pressure homogenisation equipment on nanodispersions characteristics. Int J Pharm 196:183–185

Liu J, Hu W, Chen H, Ni Q, Xu H, Yang X (2007) Isotretinoin-loaded solid lipid nanoparticles with skin targeting for topical delivery. Int J Pharm 328:191–195

Maindarkar SN, Raikar NB, Bongers P, Henson MA (2012) Incorporating emulsion drop coalescence into population balance equation models of high pressure homogenization. Colloids Surf A 396:63–73

McClements DJ (2005) Food emulsions principles, practices, and techniques, 2nd edn. CRC Press, Boca Raton

Mehnert W, Mäder K (2001) Solid lipid nanoparticles: production, characterization and applications. Adv Drug Deliv Rev 47:165–196

Mishra DK, Dhote V, Bhatnagar P, Mishra PK (2012) Engineering solid lipid nanoparticles for improved drug delivery: promises and challenges of translational research. Drug Deliv Transl Res 2:238–253

Mohr K-H (1987a) High-pressure homogenization. Part I. Liquid–liquid dispersion in turbulence fields of high energy density. J Food Eng 6:177–186

Mohr K-H (1987b) The influence of cavitation on liquid–liquid dispersion in turbulence fields of high energy density. J Food Eng 6:311–324

Mucho M, Maincent P, Müller RH (2008) Lipid nanoparticles with a solid matrix (LNP, NLC, LDC) for oral drug delivery. Drug Dev Ind Pharm 34:1394–1405

Müller RH, Schwarz C, Zur Mühlen A, Mehnert W (1994) Incorporation of lipophilic drugs and drug release profiles of solid lipid nanoparticles (LNP). Proc Int Symp Control Release Bioact Mater 21:146

Müller RH, Maassen S, Schwarz C, Mehnert W (1997) Solid lipid nanoparticles (LNP) as potential carrier for human use: interaction with human granulocytes. J Control Release 47:261–269

Müller RH, Dingler A, Schneppe T, Gohla S (2000a) Large scale production of solid lipid nanoparticles (SLN) and nanosuspensions (DissoCubes). In: Wise D (ed) Handbook of pharmaceutical controlled release technology [e-book]. Marcel Dekker, New York, pp 359–376

Müller RH, Mäder K, Gohla S (2000b) Solid lipid nanoparticles (LNP) for controlled drug delivery—a review of the state of the art. Eur J Pharm Biopharm 50:161–177

Pardeike J, Hommoss A, Müller RH (2009) Lipid nanoparticles (LNP, NLC) in cosmetic and pharmaceutical dermal products. Int J Pharm 366:170–184

Priano L, Esposti D, Castagna G, De Medici C, Fraschini F, Gasco MR, Mauro A (2007) Solid lipid nanoparticles incorporating melatonin as new model for sustained oral and transdermal delivery systems. J Nanosci Nanotechnol 7:3596–3601

Puglia C, Blasi P, Rizza L, Schoubben A, Bonina F, Rossi C, Ricci M (2008) Lipid nanoparticles for prolonged topical delivery: an in vitro and in vivo investigation. Int J Pharm 357:295–304

Qian C, McClements DJ (2010) Formation of nanoemulsions stabilized by model food-grade emulsifiers using high-pressure homogenization: factors affecting particle size. Food Hydrocoll 25:1000–1008

Saheki A, Seki J, Nakanishi T, Tamai I (2012) Effect of back pressure on emulsification of lipid nanodispersions in a high-pressure homogenizer. Int J Pharm 422:489–494

Salmaso S, Elvassore N, Bertucco A, Caliceti P (2009) Production of solid lipid submicron particles for protein delivery using a novel supercritical gas-assisted melting atomization process. J Pharm Sci 98:640–650

Schäfer-Korting M, Mehnert W, Korting HC (2007) Lipid nanoparticles for improved topical application of drugs for skin diseases. Adv Drug Deliv Rev 59:427–443

Schubert MA, Müller-Goymann CC (2003) Solvent injection as a new approach for manufacturing lipid nanoparticles—evaluation of the method and process parameters. Eur J Pharm Biopharm 55:125–131

Sebti T, Amighi K (2006) Preparation and in vitro evaluation of lipidic carriers and fillers for inhalation. Eur J Pharm Biopharm 63:51–58

Severino P, Santana MHA, Souto EB (2012) Optimizing LNP and NLC by 2^2 full factorial design: effect of homogenization technique. Mater Eng C 32:1375–1379

Sinha VR, Srivastava S, Goel H, Jindal V (2010) Solid lipid nanoparticles (SLN'S)—trends and implications in drug targeting. Int J Adv Pharm Sci 1:212–238

Sjöstrom B, Bergenstahl B (1992) Preparation of submicron drug particles in lecithin-stabilized o/w emulsions: I. Model studies of the precipitation of cholesteryl acetate. Int J Pharm 84:107–116

Souto EB, Müller RH (2006) Investigation of the factors influencing the incorporation of clotrimazole in LNP and NLC prepared by hot high-pressure homogenization. J Microencapsul 23:377–388

Trombino S, Cassano R, Muzzalupo R, Pingitore A, Cione E, Picci N (2009) Stearyl ferulate-based solid lipid nanoparticles for the encapsulation and stabilization beta-carotene and alpha-tocopherol. Colloids Surf B 72:181–187

Trotta M, Debernardi F, Caputo O (2003) Preparation of solid lipid nanoparticles by a solvent emulsification–diffusion technique. Int J Pharm 257:153–160

Varshosaz J, Ghaffari S, Khoshayand MR, Atyabi F, Azarmi S, Kobarfard F (2010) Development and optimization of solid lipid nanoparticles of amikacin by central composite design. J Liposome Res 20:97–104

Vitorino C, Carvalho FA, Almeida AJ, Sousa JJ, Pais AACC (2011) The size of solid lipid nanoparticles: an interpretation from experimental design. Colloids Surf B 84:117–130

Walstra P (1993) Principles of emulsion formation. Chem Eng Sci 48:333–349

Wooster TJ, Golding M, Sanguansri P (2008) Impact of oil type on nanoemulsion formation and Ostwald ripening stability. Langmuir 24:12758–12765

Zur Mühlen A, Mehnert W (1998) Drug release and release mechanism of prednisolone loaded solid lipid nanoparticles. Pharmazie 53:552–555

Zur Mühlen A, Schwarz C, Mehnert W (1998) Solid lipid nanoparticles (LNP) for controlled drug delivery–drug release and release mechanism. Eur J Pharm Biopharm 45:149–155